Redox-Active Cellulose Langmuir−Blodgett Films Containing β-Carotene as a Molecular Wire

Keita Sakakibara, Hiroshi Kamitakahara, Toshiyuki Takano, and Fumiaki Nakatsubo*

Division of Forest and Biomaterials Science, Graduate School of Agriculture, Kyoto University, Kitashirakawa Oiwake-cho, Sakyo-ku, Kyoto 606-8502, Japan

Received December 28, 2006; Revised Manuscript Received March 9, 2007

Redox-active Langmuir−Blodgett (LB) films containing dihydrophytyl ferrocenoate (DFc) and β-carotene (βC) were fabricated by use of 6-*O*-dihydrophytylcellulose (DHPC) as a matrix. A mixture of DFc−DHPC formed a stable monolayer. Atomic force microscopy images revealed that the DFc molecules were dispersed uniformly throughout the surface in the ratio DFc:DHPC = 2:8 at 30 mN m^{-1}. The DFc−DHPC monolayer was transferred successfully onto a substrate, yielding Y-type LB films. Cyclic voltammograms for the DFc−DHPC LB films on an indium tin oxide (ITO) electrode exhibited a well-defined surface wave. The voltammograms of the DFc−DHPC LB films exhibited 60−40% redox-active ferrocene moieties, whereas those of the DFc−DHPC−βC LB films exhibited 90−70%. X-ray diffraction patterns indicated that the distance between layers was independent of βC molecules incorporated into the LB films. Consequently, these results suggested that βC can function as a molecular wire.

Introduction

Ultrathin molecular films containing chromophoric or redox moieties have been widely used to control electron transfer and excitation energy transfer. Particularly, the fabrication of photoenergy conversion systems is one of the most important issues. In such molecular organized films, spatially well-arranged moieties are an indispensable prerequisite with nanometer scale precision. For this purpose, various fabrication techniques have been applied, for example, self-assembled monolayer (SAM),[1−6] Langmuir−Blodgett (LB),[7−12] and layer-by-layer (LBL)[13−15] techniques. Among others, the LB technique has important advantages to control the film thickness by a molecular size, i.e., nanometer order, since LB films are built up by deposition of condensed monolayers at the air−water interface onto a solid substrate. Moreover, they can control the kinetics and directions of electron transfer due to the layered structure. Recently, LB films composed of polymers have received considerable attention because of their thermal and mechanical stability and less crystal transition ability in comparison to those of low molecular weight compounds such as long-alkyl-chain fatty acids.[16] For example, Miyashita et al. reported redox-active LB films composed of poly(*N*-dodecylacrylamide) bearing ferrocene moieties.[17]

Biopolymers are abundant and easily available materials in nature. In particular, cellulose is the most generous biopolymer with a stiff, shape-stable structure known for its fiber- and film-forming properties because of a strictly defined molecular structure determined by the repeating anhydroglucose unit (AGU) and strong intra- and intermolecular hydrogen bonds.[18] Among many applications, LB films of cellulose derivatives can be attractive alternatives to those of synthetic polymers. For example, Kawaguchi et al.[19] and Ito et al.[20,21] reported LB films of cellulose triester and found them to form a stable and homogeneous monolayer. Wegner and co-workers reported LB films of (trimethylsilyl)cellulose and isopentylcellulose and found that cellulose derivatives are suitable biomaterials for preparing LB films, because they consist of two essential parts, a stiff backbone and flexible side chains.[22,23] Ifuku et al. reported the highly regioselectively substituted cellulose derivatives at the 6-*O*-position also formed a homogeneous monolayer at the air−water interface and their monolayers were transferred successfully onto several substrates.[24,25] Furthermore, cellulose LB films can be extremely functional materials by incorporating guest molecules or binding functional groups covalently without destroying the regularity and homogeneity of the multilayers.[26−28]

We have focused on the fabrication of a novel biomimetic photochemical energy conversion system using a supramolecular structure of cellulose derivatives, based on the basic concept of the *role-sharing functionalization* of cellulose.[29,30] For this purpose, simplified photosynthesis systems, which include the electron-transfer model consisting of an electron acceptor (A), a photosensitizer (S), and an electron donor (D), should be incorporated into the cellulose LB films. The important point of the A−S−D multilayer systems is that these components should be well-ordered with a spatial arrangement to achieve the charge separation of electron donors and acceptors.[31,32] On the other hand, natural photosynthesis is one of the most elegant molecular devices. This is because all of the natural pigments, such as chlorophyll *a*, β-carotene, and plastoquinone, are well organized with the help of the protein matrix.[6,33,34] Cellulose has a potential to become the matrix which can anchor and arrange the functional components as an alternative to the proteins because of its molecular structure.

We have recently reported that 6-*O*-dihydrophytylcellulose (DHPC; Figure 1) is an appropriate matrix to fabricate the mixed LB films containing β-carotene (βC; Figure 1), compared with 6-*O*-stearylcellulose.[30] The dihydrophytyl side chain of DHPC is inspired from natural pigments, since the chain is assumed to be relevant for hydrophobicity, specific noncovalent interactions,[35] and high affinities for hydrophobic environments in the photosynthesis membrane.[36,37] DHPC is, therefore, a potential matrix for the functional components having the dihydrophytyl structure.

* To whom correspondence should be addressed. Phone: +81-75-753-6254. Fax: +81-75-753-6300. E-mail: tsubosan@kais.kyoto-u.ac.jp.

10.1021/bm061231m CCC: $37.00
Published on Web 04/26/2007

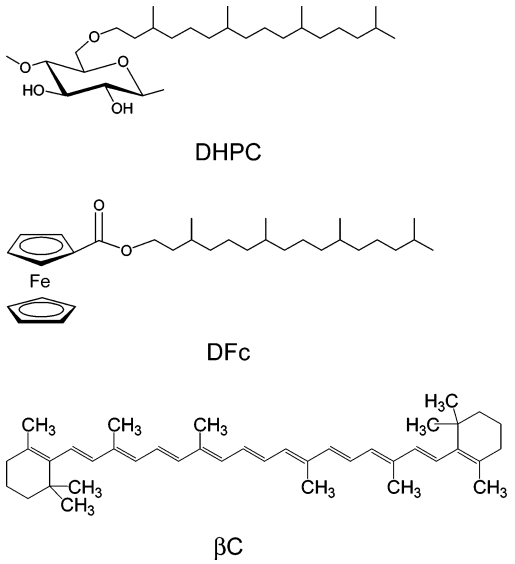

Figure 1. Chemical structures of DHPC, DFc, and βC.

We propose, herein, to use dihydrophytyl ferrocenoate (DFc; Figure 1) as an electron donor and βC as a molecular wire in the cellulose matrix for the construction of the redox-active LB films. Ferrocene is an attractive redox group known by its quasi-reversible oxidation, fairly high stability under illumination, and reductive quenching of the excited molecules.[14] Hence, DFc would properly function as an electron donor in the A−S−D system. The structure of DFc was designed to have an isoprenoid chain, so that DHPC could anchor DFc molecules with a highly ordered arrangement. We systematically studied charge quantities of ferrocene moieties in the cellulose LB films by changing the number of the layer. Furthermore, βC was incorporated into the DFc−DHPC LB films to analyze the participation of βC as a molecular wire in the electron transfer in the cellulose matrix. As implied in our previous paper,[30] βC molecules would be possible to pass a photocurrent from donors to acceptors through the cellulose LB films, because the long conjugated double bonds provide electric conduction to organic molecular layers.[38] Although there are several papers on electrical and electrochemical properties for synthetic carotenoids measured on electrode surfaces to corroborate this proposition,[38−45] those for βC itself are unprecedented, regardless of the abundance in nature. To the best of our knowledge, the availability of β-carotene as a molecular wire in the multilayer films has not been confirmed by the electrochemical analysis yet. The results would provide important fundamental data for the development of artificial photosynthesis systems by the cellulose LB films.

Experimental Section

Measurements. ^{1}H and ^{13}C NMR spectra were recorded with a Varian Inova 300 FT-NMR (300 MHz) spectrometer in chloroform-*d* with tetramethylsilane (Me_4Si) as an internal standard. Chemical shifts (δ) and coupling constants (J) are given in parts per million and hertz, respectively.

Atomic force microscopy (AFM) images of a monolayer film deposited on a freshly cleaved mica substrate at a pressure of 30 mN m^{-1} at 20 °C were performed using an NV 2000 (Olympus). Measurements were carried out in tapping mode using a tetrahedrally shaped silicon cantilever (AC240TS-C1, Olympus) with a spring constant of 2 N m^{-1}.

The ultraviolet−visible (UV−vis) spectra were measured by a Jasco V-560 spectrophotometer, using quartz substrates. X-ray diffraction (XRD) patterns for the mixed LB films were measured with an X-ray diffractometer (RINT2200V, Rigaku Co., Ltd.) with a Cu Kα line as the X-ray source.

Materials. DHPC was prepared as described previously.[30] The molecular weight and DP_n of DHPC were 2.2×10^4 and 35.9, respectively. Phytol (97%) was purchased from Aldrich and was purified on a silica gel (Wakogel C-200, Wako Pure Chemical Industries) column chromatograph eluted by ethyl acetate/*n*-hexane (1:2, v/v) before use. The other reagents were purchased from Nakarai Tesque, Inc. (Kyoto, Japan) or Wako Pure Chemical Industries, Ltd. (Osaka, Japan). DFc was synthesized by the following procedure. To a solution of dihydrophytol[46] (100 mg, 0.35 mmol) in THF (1 mL) were added ferrocenecarbonyl chloride (170 mg, 0.69 mmol)[47] and pyridine (0.28 mL) at 0 °C under a light shielding. The reaction mixture was stirred at room temperature overnight. The mixture was diluted with ethyl acetate, washed with water and brine, dried over Na_2SO_4, and concentrated in vacuo to afford a yellow oil. The oil was purified on a silica gel column eluted with dichloromethane to give DFc as an orange oil (160 mg, 0.31 mmol) in nearly quantitative yield. ^{1}H NMR (300 MHz, $CDCl_3$): δ 0.83−0.88 (15H, 3s, dihydrophytyl $-CH_3$), 0.97−1.80 (24H, m, dihydrophytyl H), 4.20 (5H, s, unsubstituted Cp (cyclopentadienyl) ring), 4.25 (2H, t, $-OCH_2-$), 4.38 (2H, t, substituted Cp ring), 4.80 (2H, t, substituted Cp ring). ^{13}C NMR (75 MHz, $CDCl_3$): δ 19.6, 19.7 (dihydrophytyl $-CH_3$), 22.6, 22.7, 24.4, 24.8, 28.0, 30.0, 32.8, 35.7, 35.9, 37.3, 37.4, 39.3 (dihydrophytyl $-CH_2-$, $-CH-$) 62.7 (dihydrophytyl$-OCH_2-$), 69.7, 70.1, 71.1, 71.5 (Cp ring), 171.8 (C═O).

Preparation of the LB Mono- and Multilayer Films. A diluted solution of DHPC (1×10^{-3} M with respect to AGUs) in chloroform/methanol (20:1, v/v) and those of DFc and βC in chloroform (1×10^{-3} M) were prepared and mixed at several ratios at a concentration of approximately 1×10^{-3} M. The solution filtered through a 0.5 μm syringe filter (DISMIC-03JP050AN, Advantec) was spread onto a water subphase in a Teflon-coated Langmuir trough (100 × 250 × 5 mm, FSD-300, USI-system). The ultrapure water at a normal resistance of 18.2 Ω cm (Simpli Lab, Millipore) was used for the subphase. The subphase temperature was kept constant at 20 °C by a circulating thermostated water system. The surface pressure was measured using a film balance of the Wilhelmy type. After 30 min were allowed for the solvent to evaporate off, the surface pressure (π)−area (A) isotherms were measured at a constant compression rate of 6 mm min^{-1}.

For the preparation of LB films, the vertical dipping method was used to deposit the surface monolayer onto a substrate. During the deposition, the surface pressure was controlled to 30 mN m^{-1} and the surface temperature was kept at 20 °C. Dipping speeds of the upward or downward stroke were 10 mm min^{-1} together. The solution was spread onto the subphase after the substrate was immersed. The initial monolayer was transferred onto the substrate by withdrawing a plate immersed in the subphase through the monolayer at the air−water interface. The successive monolayers were constantly transferred onto the substrate at both lifting/dipping processes.

Quartz plates (for UV), indium tin oxide (ITO; Geomatec) electrodes (for cyclic voltammetry), and glass plates (for XRD) were employed as substrates for the monolayer deposition. They were cleaned in a 5% aqueous detergent (Scat-20X-N, Nakarai Tesque Inc.) for 24 h and then placed in H_2O, acetone, chloroform, acetone, and then water in an ultrasonic bath for 15 min each.

Electrochemical Measurements. Electrochemical measurements of the mixed LB films deposited on an ITO electrode were carried out in a conventional three-electrode configuration using a saturated calomel electrode (SCE) as the reference electrode and a platinum wire as the counter electrode. All measurements were performed at room temperature (approximately 25 °C) using an electrochemical analyzer (ALS650B, BAS). A solution of $NaClO_4$ (1 M) was used as the supporting electrolyte solution. Oxygen was removed from the solutions by bubbling nitrogen for at least 15 min before electrochemical measurements. The working electrode area of 0.78 cm^2 was exposed to the electrolyte solution.

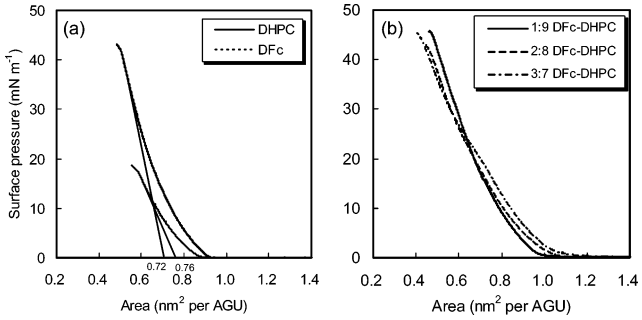

Figure 2. $\pi-A$ isotherms of (a) pure DHPC and DFc monolayers and (b) the DFc−DHPC monolayers mixed at various molar ratios at the air−water interface at 20 °C.

Table 1. Monolayer Properties of DFc−DHPC Mixtures

mixture ratio DFc:DHPC	surface area[a] (nm^2 molecule^{-1})	collapse pressure (mN m^{-1})	roughness[b] (nm)
0:1	0.72	43	0.122
1:9	0.80	45	0.134
2:8	0.81	44	0.157
3:7	0.85	45	0.186
1:0	0.76	18	-

[a] Limiting surface area estimated by extrapolating the steepest part of the isotherm to zero surface pressure. [b] rms surface roughness of the mixed monolayer transferred at 30 mN m^{-1} onto freshly cleaved mica at 20 °C.

Results and Discussion

***$\pi-A$* Isotherms of Mixed Monolayers of DHPC and DFc.** The formation of a monolayer from a mixture of DHPC and DFc in several molar proportions on the water surface was investigated by $\pi-A$ isotherm measurements at 20 °C (Figure 2). The $\pi-A$ isotherm for pure DHPC gives a steep increase and exhibits a high collapse pressure without phase transition, as described in our previous paper.[30] On the contrary, the monolayer of pure DFc collapsed at a low pressure of 18 mN m^{-1}. This indicates a low surface stability of DFc at the air−water interface: it is difficult to prepare a stable pure DFc monolayer. The limiting molecular area of pure DFc is almost 0.76 nm^2 per molecule by the extrapolation of the steepest part of the isotherm to zero surface pressure (Table 1). This value is larger than the cross-section area of the ferrocene head group (ca. 0.5 nm^2),[1,7] suggesting the observed area is obviously due to the dihydrophytyl group.

To create a stable monolayer containing the ferrocene molecules, the solution of DFc was diluted with that of DHPC. The method to fabricate mixed LB films consisting of both a functional molecule and a matrix is available for the molecules which cannot form stable LB films by themselves.[48] As shown in Figure 2b, the $\pi-A$ isotherms of DFc−DHPC mixtures at various molar ratios show steep increases and exhibit high collapse pressures above 40 mN m^{-1}, indicating that DHPC assists DFc to form a stable monolayer with a highly oriented structure at the air−water interface. This is presumably because DFc molecules are anchored in the DHPC matrix with high mechanical strength. Furthermore, the DFc:DHPC = 1:9 and 2:8 mixed monolayers have no clear kink points, indicating that the two mixing components are mutually miscible.[49] On the other hand, in the ratio of 3:7, buckling was observed around 25 mN m^{-1} (Figure 2b). As discussed later, the AFM image (see Figure 4c) of the DFc:DHPC = 3:7 mixed monolayer deposited at a surface pressure of 30 mN m^{-1} was heterogeneous. Therefore, the DFc:DHPC = 3:7 mixed monolayer would be partially collapsed above the surface pressure of the kink point, 25 mN m^{-1}.

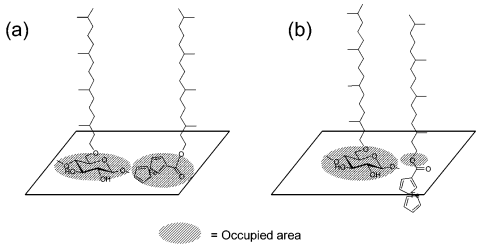

Figure 3. Schematic illustrations of the configuration of the DHPC and DFc monolayer at the air−water interface (a) below and (b) above approximately 25 mN m^{-1}.

In general, the experimentally obtained $\pi-A$ isotherms for the pure component make it possible to predict the mean molecular area in the mixed monolayer theoretically by the additive rule.[50] In Figure 2b, the isotherms of DFc−DHPC mixtures below a surface pressure of approximately 25 mN m^{-1} positively deviate from the theoretical ones and their surface areas increase in proportion to the DFc concentration. On the other hand, the isotherms of DFc−DHPC mixtures above ca. 25 mN m^{-1} exhibit the linear portion of the condensed state and their limiting surface areas approach that of DHPC: the DFc molecules do not affect the occupied area of the mixed monolayer. A similar observation was reported by Aoki and Miyashita.[17] This isotherm behavior suggests that the bulky ferrocene moiety was squeezed into the water phase and occupied no surface area at the air−water interface in the monolayer film,[17] as shown in Figure 3. It may be concluded that stable and condensed monolayers of the DFc−DHPC mixture were obtained at a higher pressure than 25 mN m^{-1}. Therefore, the surface pressure to deposit the mixed monolayer onto a substrate was determined to be 30 mN m^{-1}.

AFM Images of Monolayer Films. AFM provides direct information on the morphology of the surface monolayer.[20] Parts a−c of Figure 4show AFM images of the DFc−DHPC mixed monolayer films deposited onto freshly cleaved mica at 30 mN m^{-1} at different mixing ratios. In the DFc:DHPC = 1:9 and 2:8 mixed monolayer films, the images obtained were relatively smooth and homogeneous: well-ordered monolayer films were fabricated. In the DFc:DHPC = 3:7 mixed monolayer film, however, bean-shaped patches were found, suggesting the existence of different phases or aggregates due to packing differences.[51] Hence, the homogeneous monolayer cannot be prepared at 30 mN m^{-1} in the mixing ratio 3:7.

Table 1 shows the roughness of the monolayer films, defined as the root-mean-square (rms) height differences of the monolayer surface transferred at 30 mN m^{-1}. These values were gradually increased in proportion to the DFc content. On the basis of these observations, the optimum mixing ratio of DFc to DHPC to prepare homogeneous LB films was determined to be not more than 2:8 for the fabrication of redox-active cellulose LB films.

Fabrication of LB Films of DFc−DHPC. The DFc−DHPC monolayer was successfully transferred onto several substrates, such as quartz, glass plates, and ITO electrodes, at 30 mN m^{-1} at both lifting and dipping processes. Y-type LB films of DFc−DHPC were obtained. The initial monolayer was transferred onto the substrate by lifting a plate immersed in the subphase through the monolayer at the air−water interface. The transfer ratios in the upstroke and downstroke were 1.0 ± 0.05 and 0.9 ± 0.1, respectively.

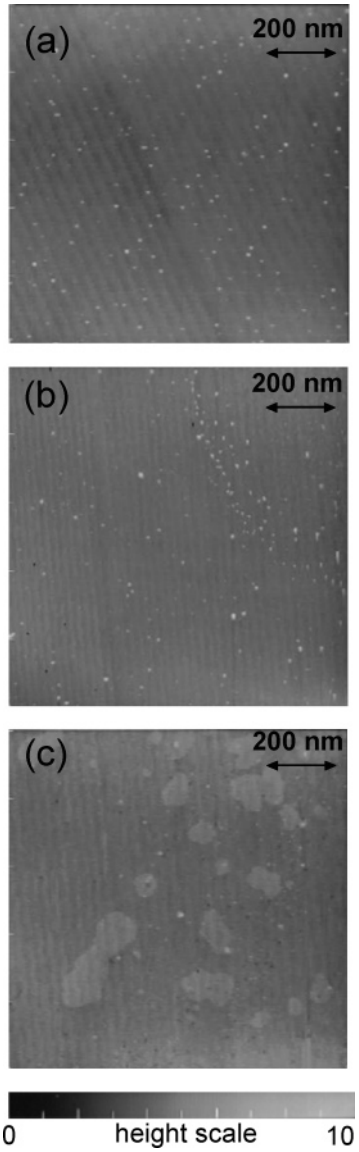

Figure 4. AFM images of the DFc−DHPC mixed monolayer films deposited onto freshly cleaved mica at a pressure of 30 mN m^{-1} at 20 °C. The mixture ratio of DFc−DHPC is (a) 1:9, (b) 2:8, and (c) 3:7.

Figure 5 shows UV−vis absorption spectra by successive measurements up to 11 layers of the deposited DFc−DHPC LB film as a function of the number of layers. The adsorption band of the ferrocene moiety was observed below 300 nm.[52,53] A linear increase demonstrates that the successive deposition of the DFc−DHPC mixed monolayer occurred by this method and that Y-type LB multilayer films were formed successfully. As a result, the mixing method can provide a stable deposition of the monolayer onto an ITO electrode, which enables us to investigate the electrochemical properties of the DFc−DHPC LB films.

Electrochemical Properties of the DFc−DHPC Monolayer Film. Figure 6a shows cyclic voltammograms in 1 M $NaClO_4$ of the DFc:DHPC = 2:8 LB monolayer film on an ITO electrode at scan rates of 10, 25, 50, 100, 200, 300, 400, 500, 600, 700, and 800 mV s^{-1}. All voltammograms showed well-defined surface waves consisting of symmetric oxidation and reduction waves. These peaks are ascribed to the oxidation of the ferrocene (Fc) and the reduction of the ferrocenium (Fc^+) moieties, respectively, in the LB film. The height of the peak increased linearly as the scan rate increased up to 300 mV s^{-1} (Figure 6b), showing that the ferrocene moieties are located on the electrode. This relationship indicates the electron transfer in the film was fast at a scan rate of less than 300 mV s^{-1}.

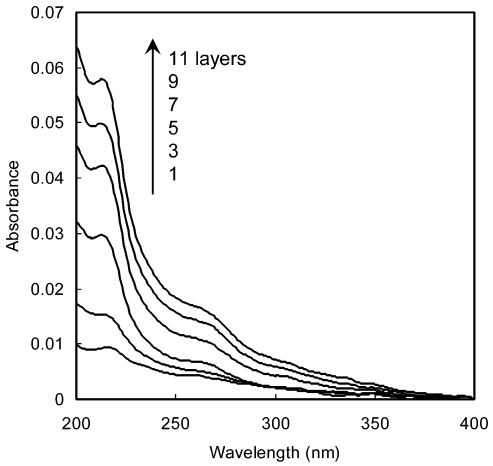

Figure 5. UV−vis absorption spectra of the DFc:DHPC = 2:8 LB films on a quartz substrate as a function of the number of deposited layers.

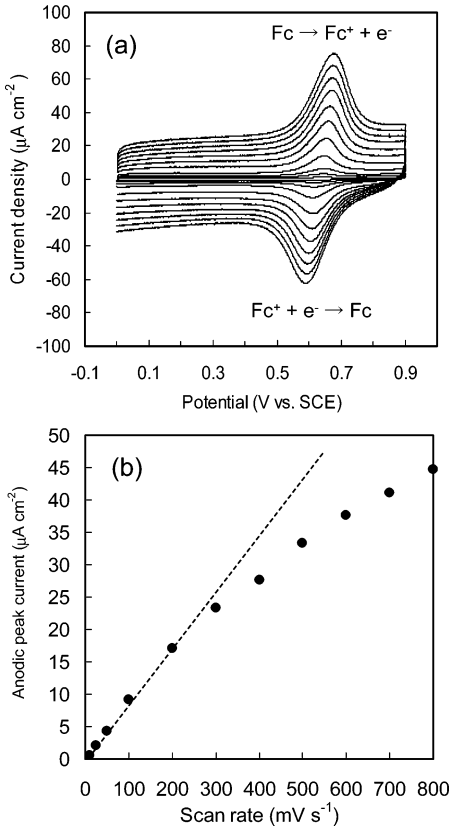

Figure 6. (a) Cyclic voltammograms for the DFc−DHPC (2:8) LB monolayer on an ITO electrode in 1 M $NaClO_4$ solution. Scan rates from the inner part to the outer part are 10, 25, 50, 100, 200, 300, 400, 500, 600, 700, and 800 mV s^{-1}. (b) Relation between the sweep rate and anodic peak current.

Table 2 lists electrochemical properties of the DFc−DHPC mixed LB films. The anodic peak position (E_{pa}) observed in the DFc−DHPC film was relatively high in contrast to that of various ferrocene derivatives on electrodes reported so far.[1,7,47,54] Chidsey et al. have reported that the ferrocene moieties in the highly ordered structure are oxidized at a more positive potential, since the repulsion among the ferrocenium moieties should be larger in the well-ordered monolayer than in the less ordered monolayer.[1] Thus, the experimental results show that the

Table 2. Electrochemical Properties of the Mixed DFc−DHPC and DFc−DHPC−βC LB Films[a]

mixture ratio DFc:DHPC:βC	no. of layers	E_{pa} (V)	E_{pc} (V)	ΔE_p[b] (mV)	$\Delta E_{1/2}$[c] (mV)	charge density (Q) (μC cm^{-2})	surface coverage (Γ) (10^{-10} mol cm^{-2})
2:8:0	1	0.649	0.615	34	98	5.58	0.58
	3	0.682	0.621	61	84	12.7	1.31
	5	0.691	0.622	69	90	18.4	1.91
	11	0.716	0.526	190	92	40.8	4.23
2:8:1	1	0.655	0.620	40	90	8.40	0.87
	3	0.670	0.620	48	80	21.3	2.21
	5	0.706	0.620	91	82	37.6	3.89
	11	0.764	0.580	184	82	71.8	7.44

[a] Sweep rate 100 mV s^{-1}. [b] Potential separation between anodic (E_{pa}) and cathodic (E_{pc}) peaks. [c] Peak width at half-height of the oxidation wave.

ferrocene moieties in the DFc−DHPC monolayer film are highly ordered. Furthermore, the monolayer film was stable against pealing off during the potential scans, since almost no variations in the cyclic voltammograms were observed after repeated successive potential scans.

At a scan rate of 100 mV s^{-1}, the potential separation between the anodic (E_{pa}) and cathodic (E_{pc}) peaks of the DFc−DHPC monolayer film ($\Delta E_p = E_{pa} - E_{pc}$) was found to be 34 mV (Table 2), indicating that the rate of electron transfer from the film to the electrode and counterion movement in the film were fast on the time scale of the experiment.[1,47,54] Only a slight increase of the peak separation at a scan rate of more than 200 mV s^{-1} was noted. The peak width at half-height of the oxidation wave ($\Delta E_{1/2}$) was 98 mV at a scan rate of 100 mV s^{-1} (Table 2), which was close to the ideal value of 90.6 mV.[55] The $\Delta E_{1/2}$ values of the copolymer LB monolayer films of *N*-dodecylacrylamide with ferrocenylmethyl acrylate transferred onto ITO electrodes, reported by Aoki and Miyashita, were 130−170 mV.[17] These values are larger than those of the DFc−DHPC monolayer film in our present paper. The width of the peak ($\Delta E_{1/2}$) is responsible for the lateral interactions between the oxidized and reduced forms in the film:[55] the distribution of the redox moieties. The $\Delta E_{1/2}$ value in the DFc−DHPC monolayer films suggests the weak interaction of the redox groups attached to the surface,[1] which led to a reasonable conclusion that DFc molecules are homogenously dispersed in the DHPC matrix. The mixing method could lead to the thermodynamically ideal behavior of the ferrocene moiety.

In general, a significant portion of the ferrocene residues at the electrode surface are not involved in the redox reaction, as described by Anzai et al.[56,57] The ratio of the redox-active ferrocene moieties in the LB films can be calculated on the basis of the adsorption coverage (Γ) compared with the ferrocene highest coverage. The adsorption coverage (Γ) can be estimated from Faraday's law

$$|Q| = nFA\Gamma \quad (1)$$

where Q, n, F, and A are the surface charge density, the number of electrons, the Faraday constant, and the area of the electrode, respectively. The surface charge density (Q) can be calculated from the integration of the oxidation peak of the cyclic voltammograms. On the other hand, the ferrocene highest coverage on the surface can be estimated by assuming that the diameter of a ferrocene moiety is calculated to be 6.6 Å and the ferrocene compound is close-packed,[1] since the occupied area at the deposition pressure (Figure 2b) does not reflect the area of the ferrocene moiety in the mixed monolayer.

The surface charge density of the DFc:DHPC = 2:8 mixed monolayer was 5.58 μC cm^{-2} (Table 2), and thus, the adsorption coverage (Γ) is estimated to be 5.78×10^{-11} mol cm^{-2}. On the other hand, the ferrocene highest coverage on the surface is estimated to be 9.7×10^{-11} mol cm^{-2} in the DFc:DHPC = 2:8 mixed monolayer. Hence, the ratio of redox-active ferrocene moieties in the monolayer film was ca. 60%. This low electroactivity would be due to the blocking of counterion permeation to the redox-active sites by the highly oriented dihydrophytyl chains, because ferrocene moieties are adsorbed to the electrode surface directly by the lifting process.

Electrochemical Properties of DFc−DHPC Multilayer Films. To discuss the interlayer electron-transfer process, cyclic voltammograms as a function of the number of deposited layers were measured. Figure 7 shows cyclic voltammograms for the DFc:DHPC = 2:8 mixed LB multilayer films. The peak current and redox potential were dependent on the number of layers (Table 2). Figure 8(○) shows the relationship between the number of layers and the anodic peak currents. As the number of deposited layers increased, the peaks became higher in proportion, indicating that ferrocene moieties in the outer layers are still redox-active as well as those located in the inner layers. The voltammograms, however, became distorted (Figure 7); that is, the potential separation (ΔE_p) increased in proportion to the thickness of the LB multilayer films (Table 2). This is because the rate of interlayer electron transfer becomes slower with increasing distance between the redox site and the electrode surface.[17] In other words, the redox reaction is apparently diffusion controlled. The copolymer LB multilayer films of *N*-dodecylacrylamide with ferrocenylmethyl acrylate also have a similar tendency,[17] indicating that it is characteristic of LB multilayer films containing a redox moiety.

The adsorption coverage (Γ) of the redox-active ferrocene moieties in the 3, 5, and 11 layers of the DFc−DHPC LB multilayer films were 1.31×10^{-10}, 1.91×10^{-10}, and 4.23×10^{-10} mol cm^{-2}, respectively (Table 2). On the other hand, the highest surface coverage of the ferrocene moieties in the 3, 5, and 11 multilayer films are 2.91×10^{-10}, 4.86×10^{-10}, and 1.07×10^{-9} mol cm^{-2}, respectively. Consequently, the ratio of the redox-active ferrocene moieties in the DFc−DHPC LB multilayer films was approximately 60−40% (Figure 9, ○). This is presumably because both the interlayer electron transfer between the LB films and the counterion movement through the monolayer film are disturbed by the dihydrophytyl chains, which behave as an insulator and/or a barrier.[57] Thus, the coverage of the redox-active ferrocene moieties in the DFc−DHPC LB multilayer films is a low-limit estimate due to the reduced electrochemical response.

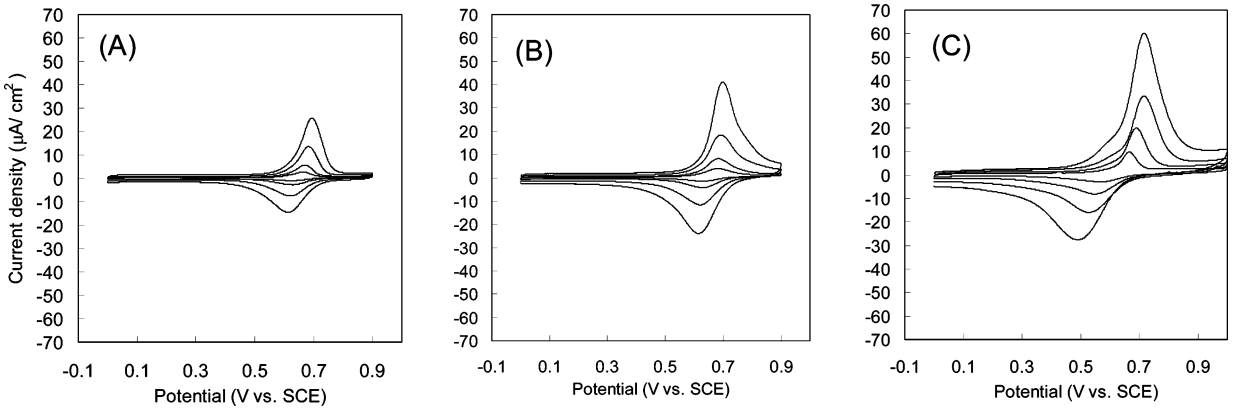

Figure 7. Cyclic voltammograms for the DFc−DHPC (2:8) LB multilayer films on ITO electrodes in 1 M $NaClO_4$ solution. Scan rates from the inner part to the outer part are 10, 25, 50, and 100 mV s^{-1}. Key: (A) three layers, (B) five layers, (C) eleven layers.

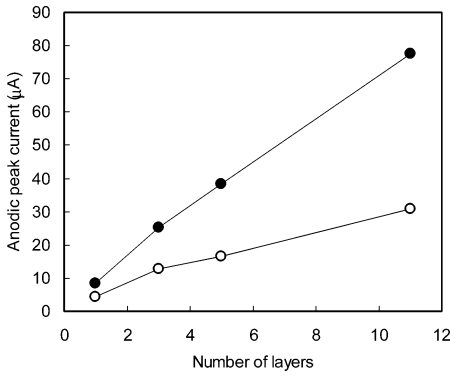

Figure 8. Anodic peak currents for 2:8 DFc−DHPC (○) and 2:8:1 DFc−DHPC−βC (●) LB multilayer films deposited onto ITO electrodes, scan rate 50 mV s^{-1}.

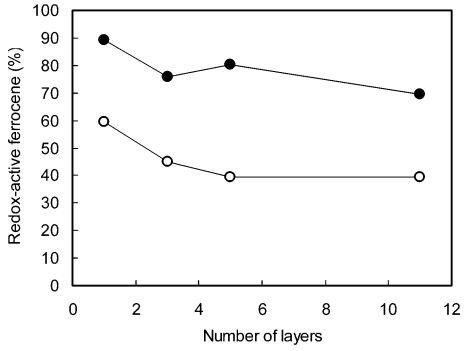

Figure 9. Ratios of redox-active ferrocene moieties in 2:8 DFc−DHPC (○) and 2:8:1 DFc−DHPC−βC (●) LB multilayer films.

One plausible way to overcome this insulating effect is to incorporate βC, which is thought to be a molecular wire with long conjugated double bonds,[44] as described in our previous paper.[30]

Effect of β-Carotene. It is desirable for the content of βC in the matrix to be around 10%, according to the results of the reference to use a synthetic carotenoid as a molecular wire.[38] The $\pi-A$ isotherm of the DFc:DHPC:βC = 2:8:1 mixed monolayer showed a steep increase and high collapse pressure, indicating that βC does not affect the formation of a stable and highly ordered monolayer. The monolayer was successively transferred at 30 mN m^{-1} on several substrates at 20 °C as a Y-type film without exfoliation.

The cyclic voltammograms of DFc:DHPC:βC = 2:8:1 monolayer and multilayer films were almost similar to that of the DFc:DHPC = 2:8 film from the viewpoint of the symmetrical surface wave shape, ΔE_p, and $\Delta E_{1/2}$. In addition, both the anodic peak current of the LB films (Figure 8, ●) and the adsorption coverage of the redox-active ferrocene moieties increased by adding βC to the DFc−DHPC LB films (Table 2). Furthermore, the ratios of redox-active ferrocene moieties in the DFc−DHPC−βC LB films were maintained around 90−70% (Figure 9, ●), although those in the DFc−DHPC films descended to 40% (Figure 9, ●). Therefore, the β-carotene molecules play an important role in increasing the ratio of redox-active ferrocene moieties. This effect should be attributed to the long conjugated double bonds of βC, resulting in electron conduction through the highly oriented dihydrophytyl chains. In addition, the ratio of redox-active ferrocene moieties rose even in the case of the monolayer containing βC (Figure 9). This is presumably because the positive charges derived from the Fc^+ moieties were transferred to βC, so that the charges were delocalized over the length of the long conjugated chain. Thus, anions in electrolyte solution, which are required to compensate for the electric charge,[3] could form an ion pair with the positively delocalized βC, since βC molecules are thought to stand on the electrode with the assistance of DHPC[30] and be in contact with the electrolyte solution directly. Consequently, it should be reasonable to suppose that βC molecules are effective in providing electron conduction to organic LB films in a direction perpendicular to an ITO substrate: it is suggested that βC can function as a molecular wire in the cellulose LB films.

The effects of the synthetic carotenoid on the electroconductivity of LB monolayer films were studied by Miyahara and Kurihara.[38] They observed that doping the monolayer with iodine provided electron conduction to the film. This iodine-doping procedure induces the carotenoid derivative to form a charge-transfer complex and/or a carbonium ion complex, so that the charges are delocalized in the long conjugated system along the polyene backbone.[38] However, in our case, the doping did not affect the conductive property of the DFc−DHPC−βC LB films. It can be assumed that this is responsible for the observation range of the redox compounds. We observed the redox peak of the ferrocene compound in the range between 0 and +1.0 V, whereas Miyahara et al. observed it in the range between −0.9 and 0 V: the electrochemical oxidation of βC, whose oxidation potential occurs around 0.6 V vs SCE,[58] should induce the formation of the radical cation and/or dication in our case.

The cyclic voltammograms of DFc:DHPC:βC = 2:8:3 LB films were almost similar to those of DFc:DHPC:βC = 2:8:1 LB films. As a result, the mixing ratio of βC around 10% is

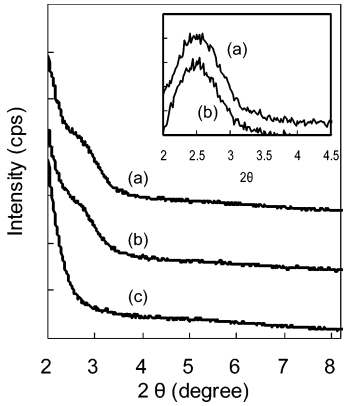

Figure 10. XRD patterns for (a) 23-layered DFc−DHPC (2:8), (b) 19-layered DFc−DHPC−βC (2:8:1) LB films, and (c) a glass plate. The inset shows differential spectra of (a) 23-layered DFc−DHPC (2:8) and (b) 19-layered DFc−DHPC−βC (2:8:1) LB films.

proved to be sufficient to improve the electrochemical property of the ferrocene moiety. On the other hand, the reduction of the ratios of redox-active ferrocene moieties by the blocking of the counterion movement is not improved yet.

XRD Patterns of LB Films. Figure 10 shows the XRD patterns of 23-layered DFc:DHPC = 2:8 and 19-layered DFc:DHPC:βC = 2:8:1 LB films. The peaks of the differential spectra shown in the inset of Figure 10 are assigned to a (001) diffraction.[29] The diffractions of the DFc−DHPC and DFc−DHPC−βC LB films were peaked at $2\theta = 2.48°$ and 2.46°, which correspond to periodic spacings of 3.54 and 3.58 nm, respectively. From these values, the thicknesses per layer were calculated to be 1.77 and 1.79 nm, respectively, in view of the Y-type film structure. On the other hand, the maximum lengths of the dihydrophytyl chain with a trans-zigzag conformation and βC are estimated to be 2.0 and 3.0 nm, respectively, as described in our previous paper (C−C distance 0.154 nm, C−C−C angle 109.28°).[30,59] Therefore, both the alkyl chains and βC in the LB films are to some extent tilted to the plane of the LB surface. The distance between layers was independent of βC molecules involved in the LB films. In general, the charge current is affected by the distance between redox species.[17] The present result, however, indicates that the addition of βC molecules does not shorten the distance of electron transfer.

Conclusions

DFc and βC were successfully incorporated into Langmuir−Blodgett films by use of DHPC as a matrix. The mixture of DFc and DHPC formed a stable and condensed monolayer with the ferrocene moieties squeezed into the water at 30 mN m^{-1}. AFM images revealed that the DFc molecules were dispersed throughout the surface in mixing ratios DFc:DHPC = 1:9 and 2:8, whereas the aggregated structures were formed in the ratio 3:7. The mixed monolayer was transferred successively onto several substrates at both lifting/dipping processes, forming Y-type LB films. Successful deposition was confirmed by UV absorption spectra. The electrochemical properties of DFc−DHPC were investigated by cyclic voltammetry. All voltammograms of the DFc−DHPC LB films showed a well-defined surface wave consisting of symmetric oxidation and reduction peaks. The ratios of the redox-active ferrocene moieties in the DFc−DHPC LB films were 60−40%, since both the interlayer electron transfer between the LB films and the counterion movement through the monolayer film are disturbed by the dihydrophytyl chains. On the other hand, the voltammograms of the DFc−DHPC−βC (2:8:1) LB films exhibited 90−70% redox-active ferrocene moieties. XRD patterns indicated that the distance between layers was independent of βC molecules involved in the LB films. These results suggest that βC acts as a molecular wire and improves the interlayer electron transfer between the LB multilayer films.

On the basis of these results, the redox-active cellulose LB films, which act as electron donor layers in the artificial photosynthesis model, were fabricated successfully. Further studies on construction of the heterodeposited A−S−D system by use of DHPC as a matrix are in progress.

Acknowledgment. We are grateful to Prof. Kenji Kano, Kyoto University, for useful discussion about electrochemical properties. This investigation was supported in part by a Grant-in-Aid for Scientific Research from the Ministry of Education, Science, and Culture of Japan (No. 17380107).

References and Notes

(1) Chidsey, C. E. D.; Bertozzi, C. R.; Putvinski, T. M.; Mujsce, A. M. *J. Am. Chem. Soc.* **1990**, *112*, 4301−4306.
(2) Lu, X.; Li, M.; Yang, C.; Zang, L.; Li, Y.; Jiang, L.; Li, H.; Jiang, L.; Liu, C.; Hu, W. *Langmuir* **2006**, *22*, 3035−3039.
(3) Uosaki, K.; Sato, Y.; Kita, H. *Langmuir* **1991**, *7*, 1510−1514.
(4) Uosaki, K.; Kondo, T.; Zhang, X.-Q.; Yanagida, M. *J. Am. Chem. Soc.* **1997**, *119*, 8367−8368.
(5) Imahori, H.; Norieda, H.; Ozawa, S.; Ushida, K.; Yamada, H.; Azuma, T.; Tamaki, K.; Sakata, Y. *Langmuir* **1998**, *14*, 5335−5338.
(6) Imahori, H.; Norieda, H.; Yamada, H.; Nishimura, Y.; Yamazaki, I.; Sakata, Y.; Fukuzumi, S. *J. Am. Chem. Soc.* **2001**, *123*, 100−110.
(7) Facci, J. S.; Falcigno, P. A.; Gold, J. M. *Langmuir* **1986**, *2*, 732−738.
(8) Goldenberg, L. M. *J. Electroanal. Chem.* **1994**, *379*, 3−19.
(9) Aoki, A.; Miyashita, T. *J. Electroanal. Chem.* **1999**, *473*, 125−131.
(10) Caminati, G.; Gabrielli, G.; Ricceri, R.; Turro, C.; Turro, N. J. *Thin Solid Films* **1996**, *284−285*, 718−722.
(11) Hosono, H.; Kaneko, M. *J. Chem. Soc., Faraday Trans.* **1997**, *93*, 1313−1319.
(12) Naito, K.; Miura, A. *J. Am. Chem. Soc.* **1993**, *115*, 5185−5192.
(13) Fushimi, T.; Oda, A.; Ohkita, H.; Ito, S. *J. Phys. Chem. B* **2004**, *108*, 18897−18902.
(14) Fushimi, T.; Oda, A.; Ohkita, H.; Ito, S. *Thin Solid Films* **2005**, *484*, 318−323.
(15) Luo, C.; Guldi, D. M.; Maggini, M.; Menna, E.; Mondini, S.; Kotov, N. A.; Prato, M. *Angew. Chem., Int. Ed.* **2000**, *39*, 3905−3909.
(16) Miyashita, T. *Prog. Polym. Sci.* **1993**, *18*, 263−294.
(17) Aoki, A.; Miyashita, T. *Macromolecules* **1996**, *29*, 4662−4667.
(18) Redl, F. X.; Köthe, O.; Röckl, K.; Bauer, W.; Daub, J. *Macromol. Chem. Phys.* **2000**, *201*, 2091−2100.
(19) Kawaguchi, T.; Nakahara, H.; Fukuda, K. *Thin Solid Films* **1985**, *133*, 29−38.
(20) Itoh, T.; Tsujii, Y.; Fukuda, T.; Miyamoto, T. *Langmuir* **1991**, *7*, 2803−2807.
(21) Itoh, T.; Tsujii, Y.; Suzuki, H.; Fukuda, T.; Miyamoto, T. *Polym. J.* **1992**, *24*, 641−652.
(22) Schaub, M.; Fakirov, C.; Schmidt, A.; Lieser, G.; Wenz, G.; Wegner, G.; Albouy, P.-A.; Wu, H.; Foster, M. D.; Majrkzak, C.; Satija, S. *Macromolecules* **1995**, *28*, 1221−1228.
(23) Schulze, M.; Seufert, M.; Fakirov, C.; Tebbe, H.; Buchholz, V.; Wegner, G. *Macromol. Symp.* **1997**, *120*, 237−245.
(24) Ifuku, S.; Kamitakahara, H.; Takano, T.; Tsujii, Y.; Nakatsubo, F. *Cellulose* **2005**, *12*, 361−369.
(25) Ifuku, S.; Nakai, S.; Kamitakahara, H.; Takano, T.; Tsujii, Y.; Nakatsubo, F. *Biomacromolecules* **2005**, *6*, 2067−2073.
(26) Mao, L.; Ritcey, A. M. *Macromol. Chem. Phys.* **2000**, *201*, 1718−1725.
(27) Ranieri, N.; Wegner, G. *Colloids Surf., A* **2000**, *171*, 65−73.
(28) Jung, S.; Angerer, B.; Löscher, F.; Niehren, S.; Winkle, J.; Seeger, S. *ChemBioChem* **2006**, *7*, 900−903.
(29) Ifuku, S.; Tsujii, Y.; Kamitakahara, H.; Takano, T.; Nakatsubo, F. *J. Polym. Sci., Part A: Polym. Chem.* **2005**, *43*, 5023−5031.
(30) Sakakibara, K.; Ifuku, S.; Tsujii, Y.; Kamitakahara, H.; Takano, T.; Nakatsubo, F. *Biomacromolecules* **2006**, *7*, 1960−1967.

(31) Nishikata, Y.; Morikawa, A.; Kakimoto, M.; Imai, Y.; Hirata, Y.; Nishiyama, K.; Fujihira, M. *J. Chem. Soc., Chem. Commun.* **1989**, 1772−1774.
(32) Fujihira, M.; Araki, T. *Bull. Chem. Soc. Jpn.* **1986**, *59*, 2375−2379.
(33) Imahori, H.; Fukuzumi, S. *Adv. Funct. Mater.* **2004**, *14*, 525−536.
(34) Itoh, T.; Yano, K.; Inada, Y.; Fukushima, Y. *J. Mater. Chem.* **2002**, *12*, 3275−3277.
(35) Pan, J.; Xu, Y.; Sun, L.; Sundström, V.; Polívka, T. *J. Am. Chem. Soc.* **2004**, *126*, 3066−3067.
(36) Buoninsegni, F. T.; Becucci, L.; Moncelli, M. R.; Guidelli, R.; Agostiano, A.; Cosma, P. *J. Electroanal. Chem.* **2003**, *550−551*, 229−240.
(37) Agostiano, A.; Catucci, L.; Colafemmina, G.; Monica, M. D.; Scheer, H. *Biophys. Chem.* **2000**, *84*, 189−194.
(38) Miyahara, T.; Kurihara, K. *J. Am. Chem. Soc.* **2004**, *126*, 5684−5685.
(39) Sereno, L.; Silber, J. J.; Otero, L.; Bohorquez, M. d. V.; Moore, A. L.; Moore, T. A.; Gust, D. *J. Phys. Chem.* **1996**, *100*, 814−821.
(40) Leatherman, G.; Durantini, E. N.; Gust, D.; Moore, T. A.; Moore, A. L.; Stone, S.; Zhou, Z.; Rez, P.; Liu, Y. Z.; Lindsay, S. M. *J. Phys. Chem. B* **1999**, *103*, 4006−4010.
(41) Fungo, F.; Otero, L.; Durantini, E. N.; Silber, J. J.; Sereno, L.; Mariño-Ochoa, E.; Moore, T. A.; Moore, A. L.; Gust, D. *J. Phys. Chem. B* **2001**, *105*, 4783−4790.
(42) Liu, D.; Szulczewski, G. J.; Kispert, L. D.; Primak, A.; Moore, T. A.; Moore, A. L.; Gust, D. *J. Phys. Chem. B* **2002**, *106*, 2933−2936.
(43) Ion, A.; Partali, V.; Sliwka, H.-R.; Banica, F. G. *Electrochem. Commun.* **2002**, *4*, 674−678.
(44) Visoly-Fisher, I.; Daie, K.; Terazono, Y.; Herrero, C.; Fungo, F.; Otero, L.; Durantini, E.; Silber, J. J.; Sereno, L.; Gust, D.; Moore, T. A.; Moore, A. L.; Lindsay, S. M. *Proc. Natl. Acad. Sci. U.S.A.* **2006**, *103*, 8686−8690.
(45) Ramachandran, G. K.; Tomofohr, J. K.; Li, J.; Sankey, O. F.; Zarate, X.; Primak, A.; Terazono, Y.; Moore, T. A.; Moore, A. L.; Gust, D.; Nagahara, L. A.; Lindsay, S. M. *J. Phys. Chem. B* **2003**, *107*, 6162−6169.
(46) Ishiwatari, M.; Yamada, K.; Ishiwatari, R. *Chem. Lett.* **2000**, *2000*, 206−207.
(47) Xue, C.; Chen, Z.; Wen, Y.; Luo, F.-T.; Chen, J.; Liu, H. *Langmuir* **2005**, *21*, 7860−7865.
(48) Zhang, Z.; Nakashima, K.; Verma, A. L.; Yoneyama, M.; Iriyama, K.; Ozaki, Y. *Langmuir* **1998**, *14*, 1177−1182.
(49) Nakagawa, M.; Handa, T. *Bull. Chem. Soc. Jpn.* **1976**, *49*, 880−885.
(50) Cadenhead, D. A.; Müller-Landau, F. *J. Colloid Interface Sci.* **1980**, *78*, 269−270.
(51) Zhao, L.; feng, S.-S. *J. Colloid Interface Sci.* **2006**, *300*, 314−326.
(52) Deschenaux, R.; Megert, S.; Zumbrunn, C.; Ketterer, J.; Steiger, R. *Langmuir* **1997**, *13*, 2363−2372.
(53) Hsu, Y.; Penner, T. L.; Whitten, D. G. *Langmuir* **1994**, *10*, 2757−2765.
(54) Goldenberg, L. M.; Cooke, G.; Petty, M. C. *Mater. Sci. Eng., C* **1998**, *5*, 281−284.
(55) Bard, A. J.; Faulkner, L. R. John Wiley & Sons: New York, 2001.
(56) Liu, A.; Anzai, J.-i. *Langmuir* **2003**, *19*, 4043−4046.
(57) Sato, H.; Anzai, J.-i. *Biomacromolecules* **2006**, *7*, 2072−2076.
(58) Hapiot, P.; Kispert, L. D.; Konovalov, V. V.; Savénant, J.-M. *J. Am. Chem. Soc.* **2001**, *123*, 6669−6677.
(59) Matsuura, T.; Nishimura, A.; Shimoyama, Y. *Jpn. J. Appl. Phys.* **2000**, *39*, 3557−3561.

BM061231M